The scalar mesons in multi-channel $\pi\pi$ scattering and decays of the ψ and Υ families

Yurii S. Surovtsev[1], Petr Bydžovský[2], Thomas Gutsche[3], Robert Kamiński[4], Valery E. Lyubovitskij[3]*, Miroslav Nagy[5]

[1]Bogoliubov Laboratory of Theoretical Physics, Joint Institute for Nuclear Research, Dubna 141980, Russia
[2]Nuclear Physics Institute, Czech Academy of Sciences, Řež near Prague 25068, Czech Republic
[3]Institut für Theoretische Physik, Universität Tübingen, Kepler Center for Astro and Particle Physics, Auf der Morgenstelle 14, D–72076 Tübingen, Germany
[4]Institute of Nuclear Physics, Polish Academy of Sciences, Cracow 31342, Poland
[5]Institute of Physics, Slovak Academy of Sciences, Bratislava 84511, Slovak Republic

The f_0 mesons are studied in a combined analysis of data on isoscalar S-wave processes $\pi\pi \to \pi\pi, K\overline{K}, \eta\eta$ and on decays $J/\psi \to \phi(\pi\pi, K\overline{K})$, $\psi(2S) \to J/\psi(\pi\pi)$ and $\Upsilon(2S) \to \Upsilon(1S)\pi\pi$ from the Argus, Crystal Ball, CLEO, CUSB, DM2, Mark II, Mark III, and BESIII Collaborations. The method of analysis, based on analyticity and unitarity and using an uniformization procedure, is set forth with some details. Some spectroscopic implications from results of the analysis are discussed.

1 Introduction

The problem of scalar mesons, particularly their nature, parameters, and status of some of them, is still not solved [1]. In the 3-channel analyses of $\pi\pi$ scattering, based on the uniformizing variable [2, 3], we obtained parameters of the $f_0(600)$ and $f_0(1500)$ which considerably differ from results of analyses utilizing other methods (mainly based on dispersion relation and Breit-Wigner approaches). Reasons for this difference were understood in Refs. [4, 5]. We showed that studying wide multi-channel resonances the Riemann-surface structure of the S-matrix of considered processes must be allowed for properly. For the scalar states this should be at least the 8-sheeted Riemann surface. This is related to a necessity to analyze jointly coupled processes $\pi\pi \to \pi\pi, K\overline{K}, \eta\eta$ because analyzing only $\pi\pi$ scattering it is impossible to obtain correct parameters for the scalar states. One can conclude: Even if a wide state does not decay into a channel which opens above its mass but it is strongly connected with this channel, one ought to consider this state taking into account the Riemann-surface sheets related to the threshold branch-point of this channel. I.e., the standard dispersion relation approach, in which amplitudes are considered on the 2-sheeted Riemann surface, does not suit for a correct determination of resonance parameters. These conclusions are important because our approach is based only on the demand for analyticity and unitarity of amplitude and using an uniformization procedure. The construction of the amplitude is essentially free from any dynamical (model) assumptions utilizing only the *mathematical* fact that a local behaviour of

---

*On leave of absence from the Department of Physics, Tomsk State University, 634050 Tomsk, Russia

analytic functions determined on the Riemann surface is governed by the nearest singularities on all corresponding sheets. Therefore, our approach permits us to omit theoretical prejudice in extracting the resonance parameters.

Analyzing only $\pi\pi \rightarrow \pi\pi, K\overline{K}, \eta\eta(\eta\eta')$ [3] we showed that data on the $\pi\pi$ scattering below 1 GeV admit two sets of parameters of the $f_0(600)$: in both cases $m_\sigma \approx m_\rho$ and the total widths about 600 and 950 MeV – solutions "A" and "B", respectively. For the states $f_0(1370)$, $f_0(1500)$ (as a superposition of a broad and narrow state) and $f_0(1710)$, we got four possible scenarios of representation by poles and zeros on the Riemann surface giving similar description of the above processes and, however, quite different parameters of some resonances. E.g., in A solution we got the following spread of the masses and total widths for the $f_0(600)$, $f_0(1370)$ and $f_0(1710)$, respectively: 605-735 and 567-686 MeV, 1326-1404 and 223-345 MeV, and 1751-1759 and 118-207 MeV. Adding the data on $J/\psi \rightarrow \phi(\pi\pi, K\overline{K})$ from the Mark III, DM2 and BESIII [6], we could diminished the number of possible scenarios [5]. Moreover, *the di-pion mass distribution of $J/\psi \rightarrow \phi\pi\pi$ of the BESIII data from the threshold to about 850 MeV prefers the solution with the wider $f_0(600)$ state – B-solution.* This is a problem because most of physicists [1] prefer the narrower $f_0(600)$. Therefore, we extend our analysis adding also data on $\psi(2S) \rightarrow J/\psi(\pi\pi)$ and $\Upsilon(2S) \rightarrow \Upsilon(1S)\pi\pi$ from the Argus, Crystal Ball, CLEO, CUSB, and Mark II collaborations [7, 8].

There are also problems related to interpretation of scalar mesons, e.g., as to an assignment of the scalar mesons to $q\bar{q}$ nonets. A number of properties of these states do not allow one simply to make up this. The main problem is a discordance of the approximately equal masses of the $f_0(980)$ and $a_0(980)$ and observed $s\bar{s}$ dominance in the wave function of the $f_0(980)$. If these states are in the same nonet, then the $f_0(980)$ must be heavier than $a_0(980)$ by 250-300 MeV because the difference of the s- and u-quark masses is 120-150 MeV. Due to this fact, various solutions are proposed. The most popular variant is the 4-quark interpretation of the $f_0(980)$ and $a_0(980)$ mesons, in favour of which as though additional arguments have been found based on interpretation of the data on $\phi \rightarrow \gamma\pi^0\pi^0, \gamma\pi^0\eta$ [9]. However, the 4-quark model, beautifully solving the old problem of the unusual properties of scalar mesons, sets new questions. Where are the 2-quark states, their radial excitations and the other members of 4-quark multiplets $9, 9^*, 36$ and 36^*, which are predicted to exist below 2.5 GeV [10]? We proposed our way to solve this problem.

Further we shall consider mainly the 3-channel case because this is a minimal number of channels needed for obtaining correct values of parameters of the scalar resonances.

2   Method of the uniformizing variable

Our model-independent method which essentially utilizes a uniformizing variable can be used only for the 2- and the 3-channel cases [2, 3]. The 3-channel S-matrix is determined on the 8-sheeted Riemann surface. The matrix elements S_{ij}, where $i, j = 1, 2, 3$ denote channels, have the right-hand cuts along the real axis of the s complex plane (s is the invariant total energy squared), starting with the channel thresholds s_i, and the left-hand cuts related to the crossed channels. The Riemann-surface sheets, denoted by the Roman numbers, are numbered according to the signs of analytic continuations of the square roots $\sqrt{s - s_i}$ as follows: signs $\left(\text{Im}\sqrt{s - s_1}, \text{Im}\sqrt{s - s_2}, \text{Im}\sqrt{s - s_3} \right) = +++, -++, --+, +-+, +--, ---,$ $-+-, ++-$ correspond to sheets I, II,$\cdots$, VIII, respectively.

In the upper part of Fig. 1, the right-hand cuts of the 3-channel S-matrix are shown on the s-plane. The lower part shows how the Riemann sheets are sewed together. E.g., sheet I is sewed with sheet II, III, and VI between the thresholds $\pi\pi$ and $K\overline{K}$, $K\overline{K}$ and $\eta\eta$, and above the $\eta\eta$ threshold, respectively. Our approach is based on analyticity and unitarity and realizes an idea of the consistent account of the nearest (to the physical region) singularities on all sheets of the Riemann surface of the S-matrix, thus giving a chance to obtain a model-independent information on resonances from the data analysis. The main model-independent contribution of resonances is given by poles and corresponding zeros on the Riemann surface. A simple description of the background is a criterion of correctness of this statement.

If a resonance has the only decay mode (1-channel case), a general statement about the amplitude is that for energies in proximity of the resonance energy it describes the propagation of resonance as if it is a free par-

Figure 1: Sewing together the sheets of the Riemann surface.

ticle. This means that in the matrix element the resonance (in the limit of its narrow width) is represented by a pair of complex conjugate poles on sheet II and by a pair of conjugate zeros on sheet I at the same points of complex energy. This model-independent statement about the poles as the nearest singularities holds also when taking account of the finite width of a resonance and in the multi-channel case.

An arrangement of poles and zeros of a multi-channel resonance on the Riemann surface is obtained using the proved fact that on the physical sheet, the S-matrix elements can have only resonance zeros (beyond the real axis), at least, around the physical region. This allows to obtain formulas expressing analytic continuations of the S-matrix elements to all sheets in terms of those on the physical sheet [11]. To this end, let us consider the N-channel S-matrix (all are two-particle channels) determined on the 2^N-sheeted Riemann surface. The surface has the right-hand (unitary) cuts along the real axis of the s-variable complex plane (s_i, ∞) $(i = 1, 2, \cdots, N$ is a channel) through which the physical sheet is sewed together with other sheets. The branch points are at the zero channel momenta $k_\alpha = (s/4 - m_\alpha^2)^{1/2}$. For now we will neglect the left-hand cut on the Riemann surface related to the crossing-channel contributions, which, in principle, can be included in the background part of the amplitude.

It is convenient to label the sheets as follows (see, e.g., [12]): the physical sheet is denoted as L_0 and the other sheets as $L_{i_1 \cdots i_k}$ where $i_1 \cdots i_k$ is a system of subscripts of those channel-momenta k_{i_n} that change signs at analytical continuations from the physical onto the indicated sheet. Then the analytical continuation of S-matrix elements S_{ik} to the unphysical sheet $L_{i_1 \cdots i_k}$ is $S_{ik}^{(i_1 \cdots i_k)}$. We obtain the formula for $S_{ik}^{(i_1 \cdots i_k)}$ expressed in terms of $S_{ik}^{(0)}$ (the matrix elements S_{ik} on the physical sheet L_0), using the reality property of the analytic functions and the N-

channel unitarity. The direct derivation of these formulas requires rather bulky algebra. It can be simplified if we use Hermiticity of the K-matrix.
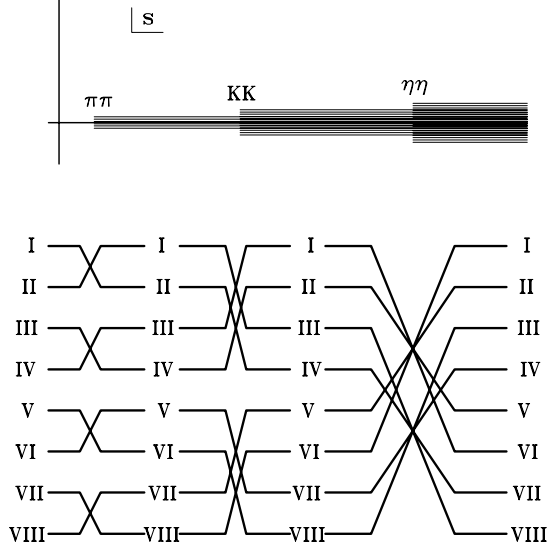
First, let us introduce the notation: $\mathbf{S}^{[i_1\cdots i_k]}$ is a matrix with zero matrix elements except for the rows $i_1, \cdots, i_k$, that consist of elements $S_{i_n i_m}$. In the matrix $\mathbf{S}^{\{i_1\cdots i_k\}}$, on the contrary, the rows $i_1, \cdots, i_k$ are zeros. Therefore, $\mathbf{S}^{[i_1\cdots i_k]} + \mathbf{S}^{\{i_1\cdots i_k\}} = \mathbf{S}$. Further we introduce the diagonal matrices $\mathbf{\Delta}^{[i_1\cdots i_k]}$ and $\mathbf{\Delta}^{\{i_1\cdots i_k\}}$ with the diagonal elements

$$\Delta_{ii}^{[i_1\cdots i_k]} = \begin{cases} 1 & \text{if } i \in (i_1\cdots i_k), \\ 0 & \text{for remaining } i, \end{cases} \quad \text{and} \quad \Delta_{ii}^{\{i_1\cdots i_k\}} = \begin{cases} 0 & \text{if } i \in (i_1\cdots i_k). \\ 1 & \text{for remaining } i, \end{cases}$$

Further using relation of the S- and K-matrices

$$\mathbf{S} = \frac{I + i\rho^{1/2}\mathbf{K}\rho^{1/2}}{I - i\rho^{1/2}\mathbf{K}\rho^{1/2}} \quad \text{where } \rho_{ij} = 0 \ (i \neq j), \ \rho_{ii} = 2k_i/\sqrt{s} \tag{1}$$

and $\mathbf{SS}^+ = \mathbf{I}$, it is easy to obtain $\mathbf{K} = \mathbf{K}^+$, i.e., the K-matrix has no discontinuity when crossing the two-particle unitary cuts and has the same value in all sheets of the Riemann surface. Using the latter fact, we obtain the needed formula. The analytical continuations of the S-matrix to the sheet $L_{i_1\cdots i_k}$ will be represented as

$$\mathbf{S}^{(i_1\cdots i_k)} = \frac{\mathbf{S}^{(0)\{i_1\cdots i_k\}} - i\mathbf{\Delta}^{[i_1\cdots i_k]}}{\mathbf{\Delta}^{\{i_1\cdots i_k\}} - i\mathbf{S}^{(0)[i_1\cdots i_k]}}. \tag{2}$$

From eq. (2) the corresponding relations for the S-matrix elements can be derived by the formula for the matrix division. In Table 1 the result is shown for the 3-channel case. We have returned to more standard enumeration of sheets by Roman numerals I, II,...,VIII. In

Process	L_0 I	L_1 II	L_{12} III	L_2 IV	L_{23} V	L_{123} VI	L_{13} VII	L_3 VIII
$1 \to 1$	S_{11}	$1/S_{11}$	S_{22}/D_{33}	D_{33}/S_{22}	$\det S/D_{11}$	$D_{11}/\det S$	S_{33}/D_{22}	D_{22}/S_{33}
$1 \to 2$	S_{12}	iS_{12}/S_{11}	$-S_{12}/D_{33}$	iS_{12}/S_{22}	iD_{12}/D_{11}	$-D_{12}/\det S$	iD_{12}/D_{22}	D_{12}/S_{33}
$2 \to 2$	S_{22}	D_{33}/S_{11}	S_{11}/D_{33}	$1/S_{22}$	S_{33}/D_{11}	$D_{22}/\det S$	$\det S/D_{22}$	D_{11}/S_{33}
$1 \to 3$	S_{13}	iS_{13}/S_{11}	$-iD_{13}/D_{33}$	$-D_{13}/S_{22}$	$-iD_{13}/D_{11}$	$D_{13}/\det S$	$-S_{13}/D_{22}$	iS_{13}/S_{33}
$2 \to 3$	S_{23}	D_{23}/S_{11}	iD_{23}/D_{33}	iS_{23}/S_{22}	$-S_{23}/D_{11}$	$-D_{23}/\det S$	iD_{23}/D_{22}	iS_{23}/S_{33}
$3 \to 3$	S_{33}	D_{22}/S_{11}	$\det S/D_{33}$	D_{11}/S_{22}	S_{22}/D_{11}	$D_{33}/\det S$	S_{11}/D_{22}	$1/S_{33}$

Table 1: Analytic continuations of the 3-channel S-matrix elements to unphysical sheets.

Table 1, the superscript I is omitted to simplify the notation, $\det S$ is the determinant of the 3×3 S-matrix on sheet I, $D_{\alpha\beta}$ is the minor of the element $S_{\alpha\beta}$, that is, $D_{11} = S_{22}S_{33} - S_{23}^2$, $D_{22} = S_{11}S_{33} - S_{13}^2$, $D_{33} = S_{11}S_{22} - S_{12}^2$, $D_{12} = S_{12}S_{33} - S_{13}S_{23}$, $D_{23} = S_{11}S_{23} - S_{12}S_{13}$, etc.

These formulas show how singularities and resonance poles and zeros are transferred from the matrix element S_{11} to matrix elements of coupled processes. Starting from the resonance zeros on sheet I, one can obtain the arrangement of poles and zeros of resonance on the whole Riemann surface ("pole clusters"). In the 3-channel case, we obtain *7 types* of resonances corresponding to 7 possible situations when there are resonance zeros on sheet I only in S_{11} – (**a**); S_{22} – (**b**); S_{33} – (**c**); S_{11} and S_{22} – (**d**); S_{22} and S_{33} – (**e**); S_{11} and S_{33} – (**f**); S_{11}, S_{22} and S_{33} – (**g**). *A necessary and sufficient condition for existence of the multi-channel resonance is its representation by one of the types of pole clusters.* A main *model-independent*

YURII S. SUROVTSEV, PETR BYDŽOVSKÝ, THOMAS GUTSCHE, ROBERT KAMIŃSKI, . . .

contribution of resonances is given by the pole clusters and possible remaining small (*model-dependent*) contributions of resonances can be included in the background. This is confirmed further by the obtained very simple description of the background.

The cluster type is related to the nature of state. *E.g.*, if we consider the $\pi\pi$, $K\overline{K}$ and $\eta\eta$ channels, then a resonance, coupled relatively more strongly to the $\pi\pi$ channel than to the $K\overline{K}$ and $\eta\eta$ ones is described by the cluster of type (**a**). In the opposite case, it is represented by the cluster of type (**e**) (say, the state with the dominant $s\bar{s}$ component). The glueball must be represented by the cluster of type (**g**) as a necessary condition for the ideal case.

One can formulate *a model-independent test as a necessary condition* to distinguish a bound state of colorless particles (*e.g.*, a $K\overline{K}$ molecule) and a $q\bar{q}$ bound state [11, 13]. In the 1-channel case, the existence of the particle bound-state means the presence of a pole on the real axis under the threshold on the physical sheet. In the 2-channel case, existence of the bound-state in channel 2 ($K\overline{K}$ molecule) that, however, can decay into channel 1 ($\pi\pi$ decay), would imply the presence of the pair of complex conjugate poles on sheet II under the second-channel threshold without the corresponding shifted pair of poles on sheet III.

In the 3-channel case, the bound state in channel 3 ($\eta\eta$) that, however, can decay into channels 1 ($\pi\pi$ decay) and 2 ($K\overline{K}$ decay), is represented by the pair of complex conjugate poles on sheet II and by the pair of shifted poles on sheet III under the $\eta\eta$ threshold without the corresponding poles on sheets VI and VII.

According to this test, earlier we rejected interpretation of the $f_0(980)$ as the $K\overline{K}$ molecule because this state is represented by the cluster of type (**a**) in the 2-channel analysis of $\pi\pi \to \pi\pi, K\overline{K}$ and, therefore, does not satisfy the necessary condition to be the $K\overline{K}$ molecule [11].

It is convenient to use the Le Couteur-Newton relations [14]. They express the S-matrix elements of all coupled processes in terms of the Jost matrix determinant $d(k_1, \cdots, k_N) \equiv d(s)$ that is a real analytic function with the only branch-points at $k_i = 0$:

$$S_{ii}(s) = \frac{d^{(i)}(s)}{d(s)}, \qquad \begin{vmatrix} S_{i_1 i_1}(s) & \cdots & S_{i_1 i_k}(s) \\ \vdots & \vdots & \vdots \\ S_{i_k i_1}(s) & \cdots & S_{i_k i_k}(s) \end{vmatrix} = \frac{d^{(i_1 \cdots i_k)}(s)}{d(s)}. \tag{3}$$

Rather simple derivation of these relations, using the ND^{-1} representation of amplitudes and Hermiticity of the K-matrix, can be found in Ref. [12]. The real analyticity implies $d(s^*) = d^*(s)$ for all s. The unitarity condition requires further restrictions on the d-function for physical s-values which will be discussed below in the example of 3-channel S-matrix.

In order to use really the representation of resonances by various pole clusters, it ought to transform our multi-valued S-matrix, determined on the 8-sheeted Riemann surface, to one-valued function. But that function can be uniformized only on torus with the help of a simple mapping. This is unsatisfactory for our purpose. Therefore, we neglect the influence of the lowest ($\pi\pi$) threshold branch-point (however, unitarity on the $\pi\pi$ cut is taken into account). This approximation means the consideration of the nearest to the physical region semi-sheets of the Riemann surface of the S-matrix. In fact, we construct a 4-sheeted model of the initial 8-sheeted Riemann surface that is in accordance with our approach of a consistent account of the nearest singularities on all the relevant sheets. In the corresponding uniformizing variable, we have neglected the $\pi\pi$-threshold branch-point and taken into account the $K\overline{K}$- and $\eta\eta$-threshold branch-points and the left-hand branch-point at $s = 0$:

$$w = \frac{\sqrt{(s - s_2)s_3} + \sqrt{(s - s_3)s_2}}{\sqrt{s(s_3 - s_2)}} \qquad (s_2 = 4m_K^2 \text{ and } s_3 = 4m_\eta^2). \tag{4}$$

In Fig. 2 we show the representation of resonances of types (**a**), (**b**), (**c**) and (**g**) used in this analysis on the uniformization w-plane for the 3-channel-$\pi\pi$-scattering S-matrix element. Representation of other type resonances can be found in Ref. [3].
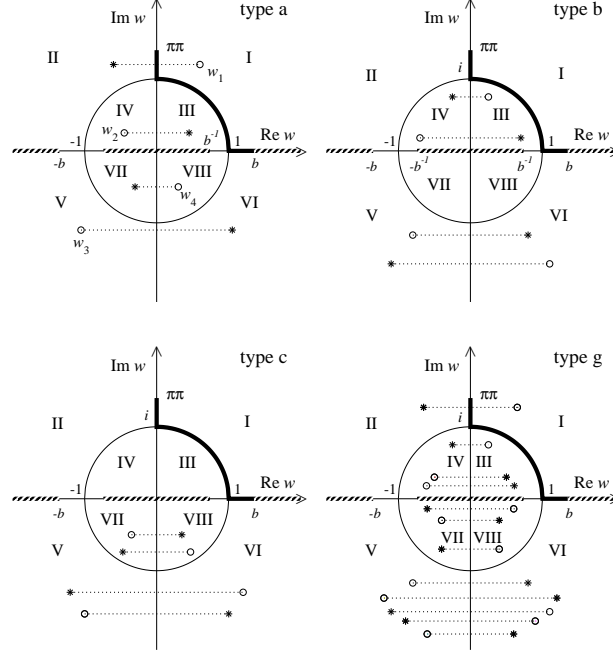
Figure 2: Uniformization w-plane. Representation of resonances of types (**a**), (**b**), (**c**) and (**g**) in S_{11} is shown.

On the w-plane, the Le Couteur–Newton relations are somewhat modified taking account of the used model of initial 8-sheeted Riemann surface:

$$S_{11} = \frac{d^*(-w^*)}{d(w)}, \qquad S_{22} = \frac{d(-w^{-1})}{d(w)}, \qquad S_{33} = \frac{d(w^{-1})}{d(w)}, \tag{5}$$

$$S_{11}S_{22} - S_{12}^2 = \frac{d^*(w^{*-1})}{d(w)}, \quad S_{11}S_{33} - S_{13}^2 = \frac{d^*(-w^{*-1})}{d(w)}, \quad S_{22}S_{33} - S_{23}^2 = \frac{d(-w)}{d(w)}. \tag{6}$$

The 3-channel unitarity requires the following relations to hold for physical w-values: $|d(-w^*)| \leq |d(w)|$, $|d(-w^{-1})| \leq |d(w)|$, $|d(w^{-1})| \leq |d(w)|$ and $|d(w^{*-1})| = |d(-w^{*-1})| = |d(-w)| = |d(w)|$.

The S-matrix elements in Le Couteur–Newton relations are taken as $S = S_B S_{res}$. The d-function is for the resonance part $d_{res}(w) = w^{-\frac{M}{2}} \prod_{r=1}^{M}(w + w_r^*)$ (M is a number of resonance zeros) and for the background part $d_B = \exp[-i\sum_{n=1}^{3}(\sqrt{s - s_n}/2m_n)(\alpha_n + i\beta_n)]$ where

$$\alpha_n = a_{n1} + a_{n\sigma}\frac{s - s_\sigma}{s_\sigma}\theta(s - s_\sigma) + a_{nv}\frac{s - s_v}{s_v}\theta(s - s_v),$$

$$\beta_n = b_{n1} + b_{n\sigma}\frac{s - s_\sigma}{s_\sigma}\theta(s - s_\sigma) + b_{nv}\frac{s - s_v}{s_v}\theta(s - s_v).$$

Here s_σ is the $\sigma\sigma$ threshold and s_v is the combined threshold of the $\eta\eta'$, $\rho\rho$ and $\omega\omega$ channels.

Di-meson mass distributions in decays $J/\psi \rightarrow \phi(\pi\pi, K\overline{K})$ and $V' \rightarrow V\pi\pi$ (e.g., $\psi(2S) \rightarrow J/\psi(\pi\pi)$ and $\Upsilon(2S) \rightarrow \Upsilon(1S)\pi\pi$) are calculated using formalism of Refs. [13]. There is assumed that pairs of pseudo-scalar mesons in final states have $I = J = 0$ and only they undergo strong interactions, whereas a final vector meson (ϕ, V) acts as a spectator. The decay amplitudes are related with the scattering amplitudes T_{ij} ($i, j = 1 - \pi\pi, 2 - K\overline{K}$) as follows:

$$F(J/\psi \rightarrow \phi\pi\pi) = \sqrt{2/3}\,[c_1(s)T_{11} + c_2(s)T_{21}], \qquad (7)$$

$$F(J/\psi \rightarrow \phi K\overline{K}) = \sqrt{1/2}\,[c_1(s)T_{12} + c_2(s)T_{22}], \qquad (8)$$

$$F(V' \rightarrow V\pi\pi \ (V = \psi, \Upsilon)) = [(d_1, e_1)T_{11} + (d_2, e_2)T_{21}] \qquad (9)$$

where $c_1 = \gamma_{10} + \gamma_{11}s$, $c_2 = \alpha_2/(s - \beta_2) + \gamma_{20} + \gamma_{21}s$, and $(d_i, e_i) = (\delta_{i0}, \rho_{i0}) + (\delta_{i1}, \rho_{i1})s$ are functions of couplings of the J/ψ, $\psi(2S)$ and $\Upsilon(2S)$ to channel i; α_2, β_2, γ_{i0}, γ_{i1}, δ_{i0}, ρ_{i0}, δ_{i1} and ρ_{i1} are free parameters. The pole term in c_2 is an approximation of possible ϕK states, not forbidden by OZI rules when considering quark diagrams of these processes. Obviously this pole should be situated on the real s-axis below the $\pi\pi$ threshold.

The expressions $\quad N|F|^2\sqrt{(s - s_i)\big(m_\psi^2 - (\sqrt{s} - m_\phi)^2\big)\big(m_\psi^2 - (\sqrt{s} + m_\phi)^2\big)}$

for $J/\psi \rightarrow \phi\pi\pi, \phi K\overline{K}$ (and the analogues ones for $V' \rightarrow V\pi\pi$) give the di-meson mass distributions. N (normalization to experiment) is 0.7512 for Mark III, 0.3705 for DM2, 5.699 for BESIII, 1.015 for Mark II, 0.98 for Crystal Ball(80), 4.3439 for Argus, 2.1776 for CLEO, 1.2011 for CUSB, and 0.0788 for Crystal Ball(85).

3 The combined 3-channel analysis of data

We performed the combined 3-channel analysis of data on isoscalar S-wave processes $\pi\pi \rightarrow \pi\pi, K\overline{K}, \eta\eta$ and on $J/\psi \rightarrow \phi(\pi\pi, K\overline{K})$, $\psi(2S) \rightarrow J/\psi(\pi\pi)$ and $\Upsilon(2S) \rightarrow \Upsilon(1S)\pi\pi$.

For the data on multi-channel $\pi\pi$ scattering we used the results of phase analyses which are given for phase shifts of the amplitudes $\delta_{\alpha\beta}$ and for the modules of the S-matrix elements $\eta_{\alpha\beta} = |S_{\alpha\beta}|$ ($\alpha, \beta = 1, 2, 3$): $S_{\alpha\alpha} = \eta_{\alpha\alpha}\exp\{2i\delta_{\alpha\alpha}\}$, $S_{\alpha\beta} = i\eta_{\alpha\beta}\exp\{i\phi_{\alpha\beta}\}$. If below the third threshold there is the 2-channel unitarity then the relations $\eta_{11} = \eta_{22}$, $\eta_{12} = (1 - \eta_{11}^2)^{1/2}$ and $\phi_{12} = \delta_{11} + \delta_{22}$ are fulfilled in this energy region.

References to used data for processes $\pi\pi \rightarrow \pi\pi, K\overline{K}, \eta\eta$ can be found in [3]. For decays $J/\psi \rightarrow \phi\pi\pi, \phi K\overline{K}$ we have taken data from Mark III, DM2 and BESIII [6]; for $\psi(2S) \rightarrow J/\psi(\pi^+\pi^-)$ from Mark II and for $\psi(2S) \rightarrow J/\psi(\pi^0\pi^0)$ from Crystal Ball Collaborations(80) [7]; for $\Upsilon(2S) \rightarrow \Upsilon(1S)(\pi^+\pi^-, \pi^0\pi^0)$ from Argus, CLEO, CUSB, and Crystal Ball Collaborations(85) [8]. In this analyses of the coupled scattering processes and decays, it is assumed that in the 1500-MeV region two states – the narrow $f_0(1500)$ and wide $f_0'(1500)$ – exist.

We have obtained the following scenarios: the $f_0(600)$ is described by the cluster of type (**a**); the $f_0(1370)$ and $f_0(1500)$, type (**c**) and $f_0'(1500)$, type (**g**); the $f_0(980)$ is represented only by the pole on sheet II and shifted pole on sheet III. However, the $f_0(1710)$ can be described by clusters either of type (**b**) or (**c**). For definiteness, we have taken type (**c**).

The resonances pole arrangement on the $\sqrt{s}$-plane can be found in [5]. The obtained background parameters are: $\underline{a_{11} = 0.0}$, $\underline{a_{1\sigma} = 0.0199}$, $\underline{a_{1v} = 0.0}$, $\underline{b_{11} = b_{1\sigma} = 0.0}$, $\underline{b_{1v} = 0.0338}$, $a_{21} = -2.4649$, $a_{2\sigma} = -2.3222$, $a_{2v} = -6.611$, $b_{21} = b_{2\sigma} = 0.0$, $b_{2v} = 7.073$, $b_{31} = 0.6421$, $b_{3\sigma} = 0.4851$, $b_{3v} = 0$; $s_\sigma = 1.6338$ GeV^2, $s_v = 2.0857$ GeV^2. The very simple description of the $\pi\pi$-scattering background (underlined values) confirms well our assumption $S = S_B S_{res}$ and

also that representation of multi-channel resonances by the pole clusters on the uniformization plane is good and quite sufficient. Moreover, this shows that *the consideration of the left-hand branch-point at $s = 0$ in the uniformizing variable solves partly a problem of some approaches (see, e.g., [15]) that the wide-resonance parameters are strongly controlled by the non-resonant background.*

Parameters of resonances and background are changed very insignificantly in comparison with our analysis in Ref. [5] performed without consideration of the $\psi(2S)$- and $\Upsilon(2S)$-decays confirming our previous results. Parameters of the coupling functions of the decay particles (J/ψ, $\psi(2S)$ and $\Upsilon(2S)$) to channel i, obtained in the analysis, are $\alpha_2, \beta_2 = 0.0843, 0.0385,$ $\gamma_{10}, \gamma_{11}, \gamma_{20}, \gamma_{21} = 1.1826, 1.2798, -1.9393, -0.9808, \delta_{10}, \delta_{11}, \delta_{20}, \delta_{21} = -0.127, 16.621, 5.983,$ $-57.653, \rho_{10}, \rho_{11}, \rho_{20}, \rho_{21} = 0.405, 47.0963, 1.3352, -21.4343.$

The data on the di-pion mass distribution in decay $J/\psi \to \phi\pi\pi$, obtained by the BESIII collaboration with rather small errors, rejects dramatically the A solution with the narrower $f_0(600)$: the corresponding curve lies considerably below the data from the threshold to about 850 MeV. Therefore in the following we will discuss mainly the B solution.

Satisfactory description of all analyzed processes is obtained with the total $\chi^2/\text{NDF} = 568.57/(481 - 65) \approx 1.37$; for the $\pi\pi$ scattering, $\chi^2/\text{NDF} \approx 1.15$; for $\pi\pi \to K\overline{K}$, $\chi^2/\text{NDF} \approx 1.65$; for $\pi\pi \to \eta\eta$, $\chi^2/\text{ndp} \approx 0.87$; for decays $J/\psi \to \phi(\pi\pi, K\overline{K})$, $\chi^2/\text{ndp} \approx 1.21$; for $\psi(2S) \to J/\psi(\pi\pi)$, $\chi^2/\text{ndp} \approx 2.43$; for $\Upsilon(2S) \to \Upsilon(1S)\pi\pi$, $\chi^2/\text{ndp} \approx 1.01$.

The combined description of the 3-channel $\pi\pi$ scattering, decays $J/\psi \to \phi(\pi\pi, K\overline{K})$ from the Mark III, DM2 and BESIII, and the data on $\psi(2S)$- and $\Upsilon(2S)$-decays is practically the same as that in Ref. [5] performed without considering decays of excited ψ- and Υ-mesons. Therefore, here we show results of fitting only to the experimental data on the $\psi(2S)$- and $\Upsilon(2S)$-decays (Figs. 3 and 4).

Generally, *wide multi-channel states are most adequately represented by pole clusters*, as the pole clusters give the main effect of resonances. The pole positions are rather stable characteristics for various models, whereas masses and widths are very model-dependent for wide resonances. However, mass values are needed in some cases, e.g., in mass relations for multiplets. We stress that such parameters of the wide multi-channel states, as *masses, total widths and coupling constants with channels, should be calculated using the poles on sheets II, IV and VIII*, because only on these sheets the analytic continuations have the forms: $\propto 1/S_{11}^{\text{I}}$, $\propto 1/S_{22}^{\text{I}}$ and $\propto 1/S_{33}^{\text{I}}$, respectively, i.e., the pole positions of resonances are at the same points of the complex-energy plane, as the resonance zeros on sheet I, and are not shifted due to the coupling of channels. E.g., if the resonance part of amplitude is taken as $T^{res} = \sqrt{s}\,\Gamma_{el}/(m_{res}^2 - s - i\sqrt{s}\,\Gamma_{tot})$, for the mass and total width, one obtains $m_{res} = \sqrt{\text{E}_r^2 + (\Gamma_r/2)^2}$ and $\Gamma_{tot} = \Gamma_r$ where the pole position $\sqrt{s_r} = \text{E}_r - i\Gamma_r/2$ must be taken on sheets II, IV, VIII, depending on the resonance classification.
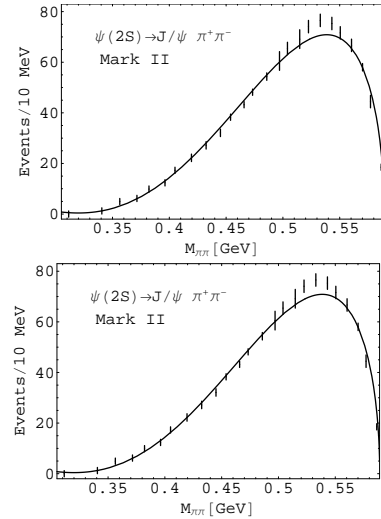
Figure 3: The $\psi(2S) \to J/\psi\pi\pi$ decays. Fitting to data [7].

Then masses and total widths are (in MeV): 693.9 ± 10.0 and 931.2 ± 11.8 for $f_0(600)$, 1008.1 ± 3.1 and 64.0 ± 3.0 for $f_0(980)$, 1399.0 ± 24.7 and 357.0 ± 74.4 for $f_0(1370)$, 1495.2 ± 3.2 and 124.4 ± 18.4 for $f_0(1500)$, 1539.5 ± 5.4 and 571.6 ± 25.8 for $f_0'(1500)$, 1733.8 ± 43.2 and 117.6 ± 32.8 for $f_0(1710)$.

4 Discussion and conclusions

In this combined analysis of data an additional confirmation of the $f_0(600)$ with mass about 700 MeV and width 930 MeV is obtained. This mass value accords with prediction ($m_\sigma \approx m_\rho$) on the basis of mended symmetry by Weinberg [16] and with an analysis using the large-N_c consistency conditions between the unitarization and resonance saturation suggesting $m_\rho - m_\sigma = O(N_c^{-1})$ [17]. Also, e.g., the prediction of a soft-wall AdS/QCD approach [18] for the mass of the lowest f_0 meson – 721 MeV – practically coincides with the value obtained in our work. Of course, such large width of this state is a problem. Maybe, we observe a superposition of two states – narrower σ-meson and wider state as it is the case in the 1500-MeV region.

Indication for $f_0(980)$ is obtained to be a non-$q\bar{q}$ state, e.g., the bound $\eta\eta$ state. The $f_0(1370)$ and $f_0(1710)$ have the dominant $s\bar{s}$ component that agrees with a number of experiments (see discussion in[3]). In the 1500-MeV region, there are two states: the $f_0(1500)$ ($m_{res} \approx 1495$ MeV, $\Gamma_{tot} \approx 124$ MeV) and the $f_0'(1500)$ ($m_{res} \approx 1539$ MeV, $\Gamma_{tot} \approx 574$ MeV). The $f_0'(1500)$ is interpreted as a glueball due to its biggest width among enclosing states [19].

We propose the following assignment of the scalar mesons to lower nonets, excluding the $f_0(980)$ as the non-$q\bar{q}$ state. The lowest nonet: the isovector $a_0(980)$, the isodoublet $K_0^*(900)$, and $f_0(600)$ and $f_0(1370)$ as mixtures of the 8th component of octet and the SU(3) singlet. The Gell-Mann–Okubo (GM-O) formula $3m_{f_8}^2 = 4m_{K_0^*}^2 - m_{a_0}^2$ gives $m_{f_8} = 870$ MeV. In relation for masses of nonet $m_\sigma + m_{f_0(1370)} = 2m_{K_0^*(900)}$ the left-hand side is by about 14% bigger than the right-hand one. For the next nonet we find: the isovector $a_0(1450)$, the isodoublet $K_0^*(1450)$, and two isoscalars $f_0(1500)$ and $f_0(1710)$. From the GM-O formula, $m_{f_8} \approx 1450$ MeV. In formula $m_{f_0(1500)} + m_{f_0(1710)} = 2m_{K_0^*(1450)}$ the left-hand side is by about 10% bigger than the right-hand one. This assignment removes a number of questions, stood earlier, and does not put any new.
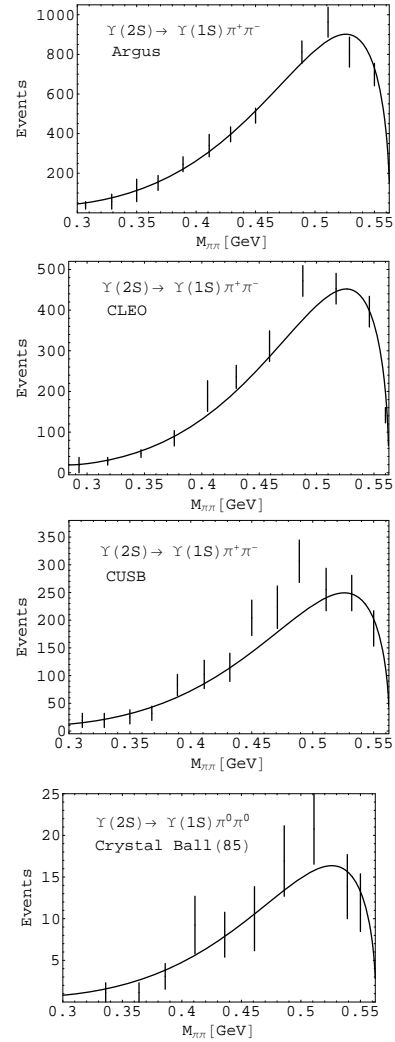
Figure 4: The $\Upsilon(2S) \to \Upsilon(1S)\pi\pi$ decays. Fitting to data [8].

References

[1] J. Beringer et al. (PDG), Phys. Rev. **D86** 010001 (2012).

[2] Yu.S. Surovtsev, P. Bydžovský, R. Kamiński, and M. Nagy, Phys. Rev. **D81** 016001 (2010).

[3] Yu.S. Surovtsev, P. Bydžovský and V.E. Lyubovitskij, Phys. Rev. **D85** 036002 (2012).

[4] Yu.S. Surovtsev, P. Bydžovský, R. Kamiński, V.E. Lyubovitskij, and M. Nagy, arXiv:1206.3438[hep-ph] (2012); Phys. Rev. **D86** 116002 (2012).

[5] Yu.S. Surovtsev, P. Bydžovský, R. Kamiński, V.E. Lyubovitskij, and M. Nagy, arXiv:1207.6937[hep-ph] (2012).

[6] W. Lockman (Mark III), Proceedings of the Hadron'89 Conference, ed. F. Binon et al. (Editions Frontières, Gif-sur-Yvette,1989) p.109; A. Falvard et al. (DM2), Phys. Rev. **D38** 2706 (1988); M. Ablikim et al. (BES III), Phys. Lett. **B607** 243 (2005).

[7] G. Gidal et al. (Mark II), Phys. Lett. **B107** 153 (1981); M. Oreglia et al. (Crystal Ball(80)), Phys. Rev. Lett. **45** 959 (1980).

[8] H. Albrecht et al. (Argus), Phys. Lett. **B134** 137 (1984); D. Gelphman et al. (Crystal Ball(85)), Phys. Rev. **D32** 2893 (1985); D. Besson et al. (CLEO), Phys. Rev. **D30** 1433 (1984); V. Fonseca et al. (CUSB), Nucl. Phys. **B242** 31 (1984).

[9] N.N. Achasov, Nucl. Phys. **A675** 279c (2000).

[10] R.L. Jaffe, Phys. Rev. **D15** 267, 281 (1977).

[11] D. Krupa, V.A. Meshcheryakov and Yu.S. Surovtsev, Nuovo Cim. **A109** 281 (1996).

[12] M. Kato, Ann. Phys. **31** 130 (1965).

[13] D. Morgan and M.R. Pennington, Phys. Rev. **D48** 1185, 5422 (1993).

[14] K.J. Le Couteur, Proc. R. London, Ser. A **256** 115 (1960); R.G. Newton, J. Math. Phys. **2** 188 (1961).

[15] N.N. Achasov and G.N. Shestakov, Phys. Rev. **D49** 5779 (1994).

[16] S. Weinberg, Phys. Rev. Lett. **65** 1177 (1990).

[17] J. Nieves and E.R. Arriola, Phys. Rev. **D80** 045023 (2009).

[18] T. Gutsche, V.E. Lyubovitskij, I. Schmidt, and A. Vega, Phys. Rev. **D87** 056001 (2013); arXiv:1212.5196 [hep-ph] (2012).

[19] V.V. Anisovich et al., Nucl. Phys. A (Proc Suppl.) **56** 270 (1997).